Nuclear Physics A540 (1992) 328–340
North-Holland

NUCLEAR
PHYSICS A

Direct versus statistical break-up processes in the $^{16,18}O+^{27}Al$, ^{28}Si reactions at $E/A \leq 4$ MeV*

N. Added, R.M. Dos Anjos, N. Carlin, L. Fante Jr., M.C.S. Figueira, R. Matheus, E.M. Szanto and A. Szanto de Toledo

Instituto de Física da Universidade de São Paulo, Departamento de Física Nuclear, Laboratório Pelletron, C.P. 20516, 01498, São Paulo, SP, Brazil

M.S. Hussein

Nuclear Theory and Elementary Particle Phenomenology Group, Instituto de Física, Universidade de São Paulo, C.P. 20516, 01498, São Paulo, SP, Brazil

C.A. Bertulani and L.F. Canto

Instituto de Física, Universidade Federal do Rio de Janeiro, 21945, Rio de Janeiro, RJ, Brazil

Received 6 August 1991

Abstract: In-plane angular correlations (C-α) were measured for the ^{27}Al, ^{28}Si ($^{16,18}O$, C-α) reactions at $E/A = 4.0$, 3.5 and 3.0 MeV. Relative energies determined for different two-body configurations indicate a competition between incomplete-fusion (ICF) and projectile-break-up (PB) processes. The analysis of the angular correlations supports this picture. Moreover, the projectile-break-up components of the measured correlations, which are mainly determined by phase-space effects, are found to be weakly sensitive to the break-up dynamics. Angular correlations predicted on the basis of a modified elastic break-up model which approximately takes into account both direct and sequential processes, were found to account well for our data.

E

NUCLEAR REACTIONS: ^{27}Al, $^{28}Si(^{16,18}O, C-\alpha)$, $E/A = 4.0$, 3.5 and 3.0 MeV. Measured E_C, E_α and $d^2\sigma/d\Omega_C\, d\Omega_\alpha$. Determined break-up and incomplete fusion yields. Direct and statistical model calculations.

1. Introduction

Mechanisms producing quasi-elastic peaks in inclusive energy spectra of projectile-like particles, as well as fast light particles have been investigated [1-3]) with increasing interest over the last few years. Studies have shown that even in the case of light heavy-ion reactions, which at moderate energies are dominated by the fusion process, non-equilibrium emission of light particles in coincidence with projectile-like fragments appears as an important feature. In the case of reactions involving nuclei as light as sd-shell nuclei, experimental difficulties appear in the characterization of the mechanism due to the fact that a given final channel can be populated

* Supported in part by CNPq and FAPESP.

via different processes. Direct [1,3]), pre-equilibrium [4,5]) and compound-nucleus [6]) reaction mechanisms can be simultaneously present down to energies of the order of the Coulomb barrier. Angular correlations were measured to shed some light on this problem. However, all the existing ambiguities have not yet been completely solved due to the difficulties which mainly arise from the high sensitivity of this type of correlation measurements to phase-space effects (geometrical constraints). Within this scenario, special attention has been paid to the ^{27}Al(^{16}O, C-α) reaction for which a controversy has arisen in the literature regarding the competition between pre-equilibrium emission [4,5]), incomplete fusion [7,8]) and projectile sequential decay [6,9]).

The analysis of the energy dependence (thresholds) of the correlations measured for projectile-like fragments detected at several angles (near the grazing angle) is expected to contribute to the solution of the ambiguities concerning the reaction dynamics.

Furthermore, models taking into account direct "elastic" break-up and sequential processes have to be developed in order to account for the data and elucidate the reaction dynamics describing the processes as two- or three-body final-states produced in the reaction. By direct "elastic" we mean the fast break-up of the projectile that leaves the target in the ground state. This is commonly denominated tidal-force break-up.

In this study we present results on the investigation of the ^{27}Al(^{16}O, ^{12}C-α), ^{27}Al(^{18}O, ^{14}C-α) and ^{28}Si(^{16}O, ^{12}C-α) reactions at bombarding energies E_{lab}(O) = 64, 56 and 48 MeV. To account for the data, a simplified DWBA-based direct break-up model has been developed. The predictions are compared to those based on a completely different approach which assumes a two-step mechanism. In this latter hybrid direct-statistical model it is assumed that an intermediate composite system is formed via a direct process which is allowed to decay statistically. This model should describe "projectile statistical break-up" processes as well as incomplete fusion followed by evaporation.

2. Experimental procedure

The experiment has been performed using oxygen beams produced by the Pelletron Accelerator [10]) of the University of São Paulo. Self-supporting ^{27}Al (1.5 mg · cm^{-2}) and ^{nat}Si (0.4 mg · cm^{-2}) targets were used.

Projectile-like and light particles were detected, both in singles and coincidence modes by (E, ΔE) telescopes [11]). Carbon particles were identified by means of a position-sensitive proportional counter (PSPC) which supplied the ΔE information. The residual energy E_R of the fragments was obtained from three silicon surface-barrier detectors, 100-200 μm thick. These detectors were fixed at 25.5°, 30.0° and 34.5° (angles on the same side as the carbon telescopes, with respect to the beam, are defined to be positive). Alpha particles were detected, in the reaction plane at

angles varying from $-100° < \theta_\alpha < +5°$ in steps of 10°, by means of another proportional counter (PC) followed by four silicon surface-barrier detectors, 1-2 mm thick. Both proportional counters used Mylar windows $\sim 250\ \mu g \cdot cm^{-2}$ thick containing 90% argon-10% methane gas at a pressure of 20-30 Torr. Typical anode voltages were 100 V. The experimental setup is shown in fig. 1. The angular separation between detectors was 10°, guaranteed by a four-slit mask located in front of the PC. Solid angles of $\Delta\Omega_C \simeq 2.5$ msr and $\Delta\Omega_\alpha \simeq 5$ msr were used for each heavy-fragment detector and each light-particle detector. In order to suppress elastically scattered particles at forward angles, and consequently decrease the dead time of the detection system, a tantalum absorber foil ($42\ mg \cdot cm^{-2}$ thick), was placed between the target and detector covering the $-20° < \theta < +20°$ angular range. A beam stopper (Ta finger blocking the $-3° < \theta < +3°$ interval) was used to stop the beam and integrate its charge. The Ta absorbers imposed a major correction to the energy of the detected light particles and to the efficiency of the detection system due to the straggling in energy and angle. The reconstruction of the primary-particle energy spectra took into account the energy losses in the target, proportional-counter windows and Ta absorber. The losses were calculated as a function of the original emission angle and angular straggling (AS). The energy loss and straggling in all these materials were estimated and taken into account also in the energy-calibration procedure, contributing with uncertainties of the order of 1 MeV in the final C-energies. The AS is responsible for the decrease of the geometrical detection efficiency observed in the data. In order to properly determine the absolute cross sections, and perform accurate energy calibration, elastically scattered $^{16,18}O$ particles on a thin ^{197}Au target, as well as evaporating α-particles, were detected with and without the Ta absorber to obtain the calibration parameters as well as the ones used in the evaluation [11,12]) of the straggling probability. Monte Carlo calculations have been

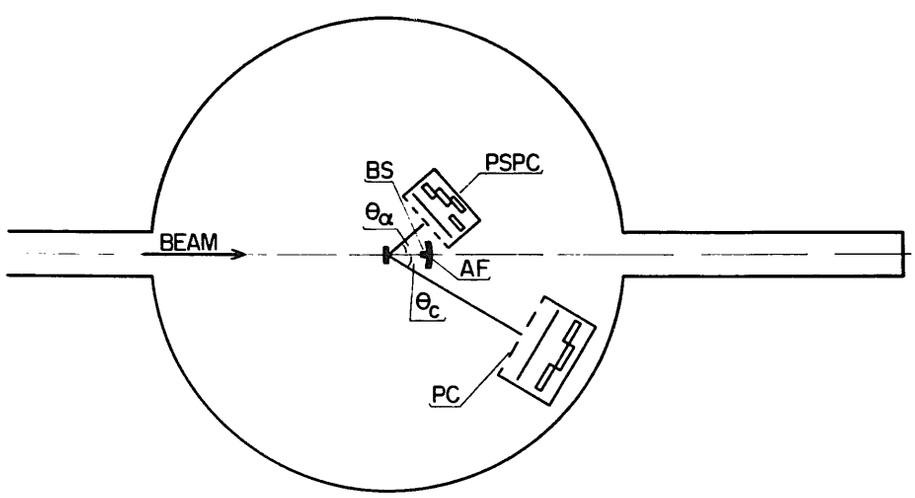

Fig. 1. Schematic diagram of the experimental set-up showing the light-particle position-sensitive proportional counter (PSPC), the projectile-like fragment detector (PC), the tantalum beam stopper (BS) and the tantalum absorber foil (AF).

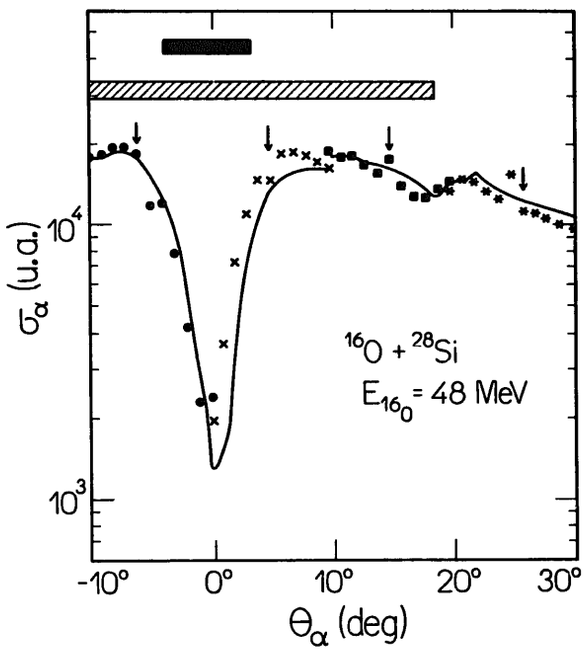

Fig. 2. Yield of α-particles observed in the $^{16}O+^{28}Si$ reaction. Different symbols represent the yield detected by different Si-detectors. Horizontal full and dashed bars describe the angular region hidden by the Ta beam stopper and Ta absorber foil, respectively. The curve represents a Monte Carlo fit to the data taking into acount the straggling effect. Vertical arrows indicate the angles at which the angular correlation data were measured.

performed in this case: a fit to the angular distribution of single α-particles is presented in fig. 2. The detection of α-particles at forward angles was perturbed by a high counting rate and consequent accidental-coincidence rates. This was due in part to the close presence of the beam stopper. Time spectra were generated by time-to-amplitude converters triggered by signals supplied by the light- and heavy-particle detectors. A clear peak was present in the time spectrum. A gate on this peak ("true gate") was used to construct the energy spectra. Accidental events were estimated by generating two new gates, "chance gates" adjacent to both sides of the "true gate". Energy spectra conditioned to the "chance gates" were subtracted from the data.

3. Experimental data

Several possible sequential or direct processes may occur in the production of α-C pairs in the final state. We may have the contribution of:

$$^{16}O+^{28}Si \begin{cases} \rightarrow (a)\ \text{Direct} \longrightarrow \\ \rightarrow (b)\ ^{16}O^*+^{28}Si \rightarrow \\ \rightarrow (c)\ ^{12}C+^{32}S^* \rightarrow \\ \rightarrow (d)\ \alpha+^{40}Ca^* \rightarrow \end{cases} \rightarrow ^{12}C+\alpha+^{28}Si$$

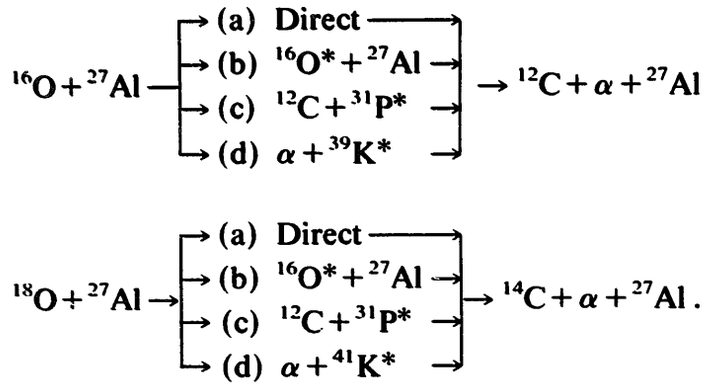

(1)

Process (a) is denominated direct break-up; (b) is denominated projectile sequential decay (PSD) and proceeds via the inelastic excitation of the projectile in a first step and the subsequent decay in the C-α channel. Processes (c) and (d), denominated incomplete fusion (ICF), evolve through the formation of an intermediate nucleus (IN) (target+α) or (target+C) which then decays back in the (target $+\alpha+$C) channel.

If the reaction proceeds in two steps via the formation of an intermediate nucleus (IN), the relative energy of the decaying fragments, in the IN rest frame, is constant. In the present work relative energies were calculated for all the events in the $^{16}O^*(^{18}O)$, $^{31}P^*$ or $^{40}Ca^*$ reference frames. In other words, if the reaction proceeds via process (b), the kinetic energy of the relative motion of C-α particles ($E^{rel}_{C-\alpha}$) deduced from the data, should be independent of the angle θ_α of the α-particle emission. Similarly, if processes (c) (or (d)) are dominant, the relative energies $E^{rel}_{\alpha-Si}$ (or E^{rel}_{C-Si}) should be angle independent. It has been shown [6,9]) that process (d) is inhibited by the high value of the Coulomb barrier in the exit channel. Kinetic energies of relative motion $E^{rel}_{C-\alpha}$ and $E^{rel}_{\alpha-Al(Si)}$ were obtained for all events. Average values were extracted and shown in fig. 3 for some cases. The results suggest that in the negative (backward) angular region, (i.e. $\theta_\alpha < -30°$) the ICF process (i.e. process (c)) is dominant for all the systems at all the energies investigated. In the angular region $\theta_\alpha > -20°$ the $E^{rel}_{\alpha-Si(\alpha)}$ is not constant and $E^{rel}_{C-\alpha}$ shows, in few cases, a tendency to constant values. It should be mentioned, however, that due to kinematical constraints [6]) the average excitation energy allowed for the intermediate nucleus varies with angle, not allowing $E^{rel}_{C-\alpha}$ to reach a constant value in the angular region measured. However, as in the case of the $^{16}O+^{28}Si$ system, (see fig. 3a) the data suggest that the projectile sequential decay contribution might be significant. This finding is further supported by the analysis of the angular correlations. Based on the saturation values of the E^{rel} values, most probable excitation energies of the intermediate nucleus can be extracted.

Angular correlations were measured for the three systems mentioned in expression (1), at three different bombarding energies i.e. $E_{lab}(0) = 64$, 56 and 48 MeV, in order to investigate the energy dependence of the several competing processes. The carbon ejectiles were detected at +25.5°, +30.0° and +34.5° in coincidence with α-particles

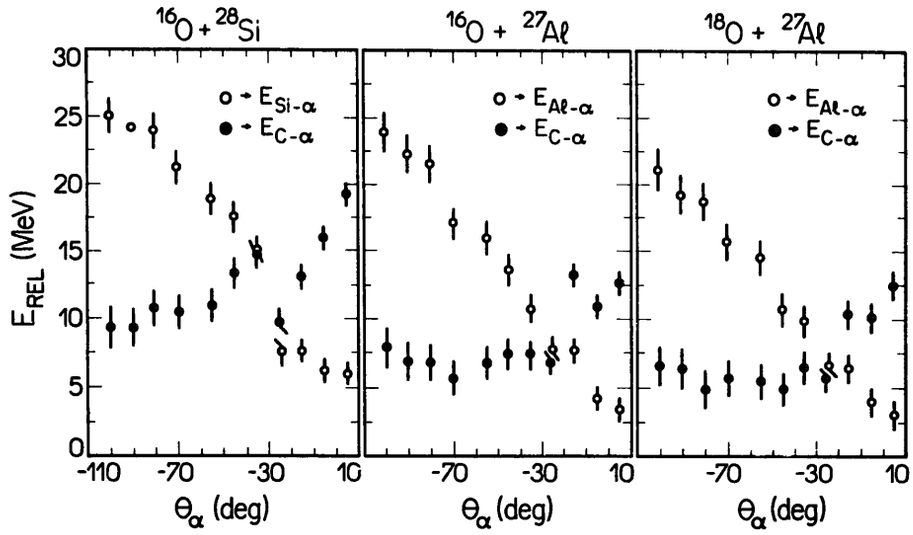

Fig. 3. Relative kinetic energies $E^{rel}_{C-\alpha}$ between α+C pairs (full circles) and $E^{rel}_{Si(Al)-\alpha}$ between target+α pairs (open circles), as a function of the α-particle detection angle θ_α. These data correspond to the case of $E_{lab} = 64$ MeV bombarding energy.

at $\theta_\alpha = -5°$, 5°, 15°, 25°, 35°, 45°, 55°, 70°, 80°, 90° and 100°. The characteristic dependence of the correlations with the angle of the detected projectile-like particles is shown in fig. 4 in the case of the $^{16}O+^{28}Si$ system. The energy dependence of the double-differential cross section $d^2\sigma/d\Omega_\alpha\, d\Omega_C$ can be seen in fig. 5 for the same system. The projectile dependence of the correlations is seen in fig. 6 for the $^{16}O+^{27}Al$ and $^{18}O+^{27}Al$ reactions at $E_{lab} = 64$ MeV.

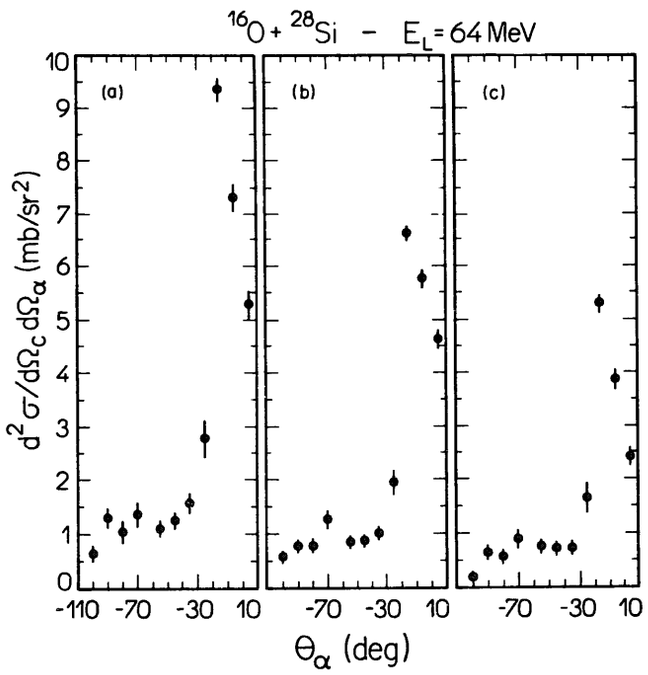

Fig. 4. In-plane angular correlations for C-α products. Carbon particles were detected at (a) $\theta_C = 25.5°$, (b) $\theta_C = 30°$ and (c) $\theta_C = 34.5°$.

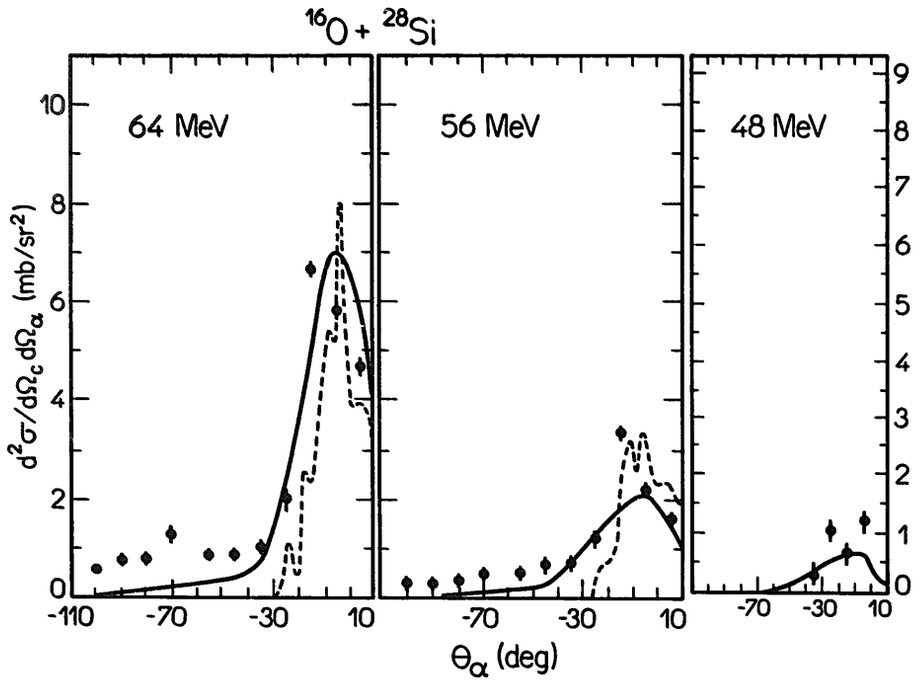

Fig. 5. In-plane angular correlations for C-α products from the $^{16}O+^{28}Si$ reaction at several energies. In these cases carbon ejectiles were detected at $\theta_C = 30°$. Solid and dashed curves correspond to theoretical predictions based on DBU and SBU model, respectively (for details see the text).

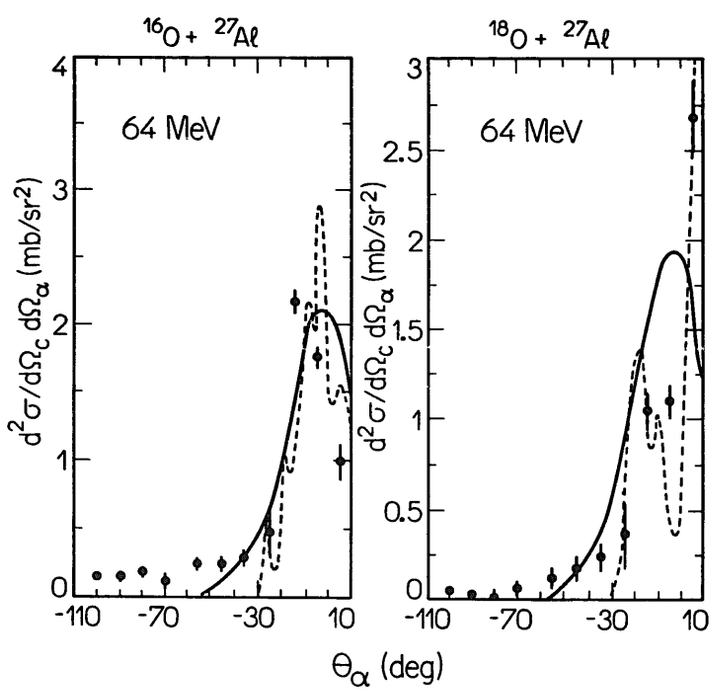

Fig. 6. In-plane angular correlations for (a) $^{16}O+^{27}Al$ reaction and (b) $^{18}O+^{27}Al$ reaction at E_{lab} = 64 MeV and $\theta_C = 30°$. Solid and dashed curves correspond to theoretical predictions based on DBU model and SBU model, respectively (for details see the text).

These correlations have very characteristic shapes independently of the system and energy. A clear peak is observed at very forward angles, which correspond to a projectile break-up process. At large negative angles, and at the highest bombarding energies, a very wide structure is observed. This structure is in fact associated with the contribution of an incomplete fusion process and supported by the observed constancy of the relative kinetic energies shown in fig. 3.

The fact that the angular correlations were measured for a wide angular range ($-100° < \theta_\alpha < +5°$) allows its integration over the θ_α variable in order to extract differential cross sections for the several processes at an angle θ_C. In order to perform this integration we assumed that the double-differential cross section $d^2\sigma/d\Omega_\alpha\, d\Omega_\alpha$ is maximum in the reaction plane and, according to data found in the literature [5]), can be associated with an out-of-plane dependence $K \cos^2 \phi$. Under this assumption the differential cross section $d\sigma/d\Omega_C(\theta_C) = \pi \int (d^2\sigma/d\Omega_\alpha\, d\Omega_C) \sin \theta_\alpha\, d\theta_\alpha$ can be estimated. Based on the fits presented in figs. 5-7, cross sections for the incomplete fusion (ICF) and break-up (BU) were extracted. The results are presented in figs. 8 and 9.

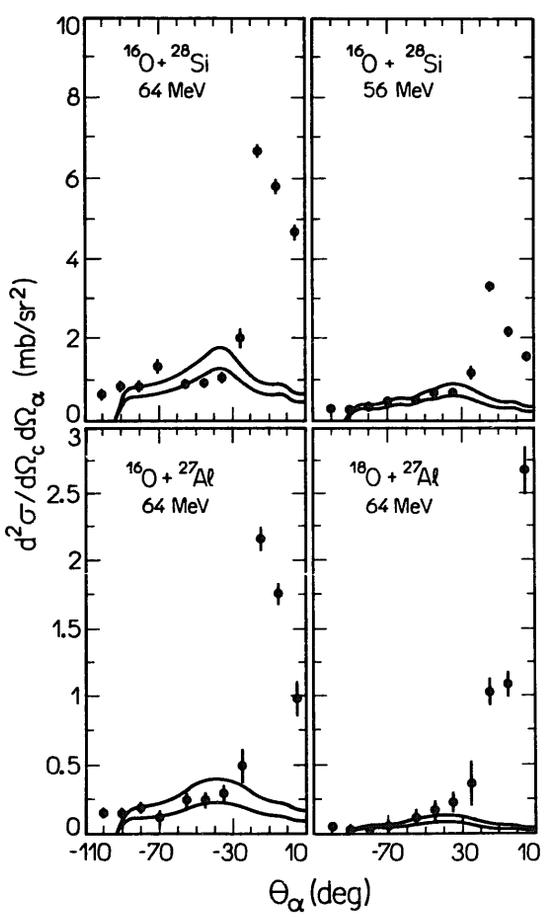

Fig. 7. Fits to the incomplete-fusion component of the angular correlation based on the ICF model described in the text. The two curves correspond to upper and lower limits according to the counting statistics of the carbon spectra.

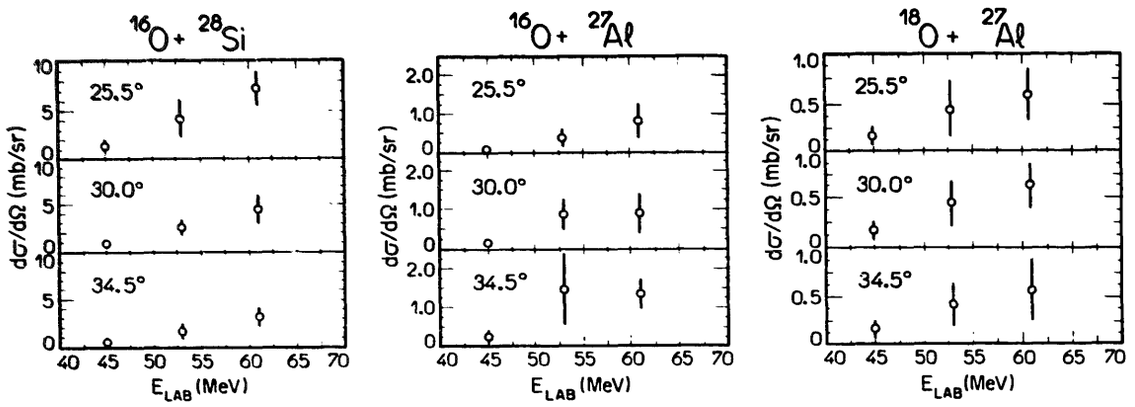

Fig. 8. Energy dependence of the incomplete fusion differential cross section $d\sigma_{ICF}/d\Omega_C$ for three different detection angles of the carbon ejectile.

4. Theoretical approaches

4.1. DIRECT "ELASTIC" BREAK-UP

According to experiments described in the literature [6,9]), the break-up of ^{16}O projectiles in experimental conditions similar to the present work is dominated by sequential decay exciting several different intermediate states of the projectiles. Therefore, one should resort to a multistep description along the lines of the next section. As is common in nuclear reaction theory, one can describe these complicated processes, on the average, as a sum of a fast, direct-like process and a slow, statistical, one. In fact, in ref. [13]) the fast component that leads from the ground state to continuum states of the $\alpha + C$ system has been suggested to account partly for the data. For our relatively low-energy events, one is required for the description of the direct process to use appropriate coupled channels, which involve the continuum states of the final three-body system and the entrance channel. However, our aim in this work is to present a comparison between the fast direct process and the statistical one. Thus, an appropriate DWBA-like calculation of the tidal force process

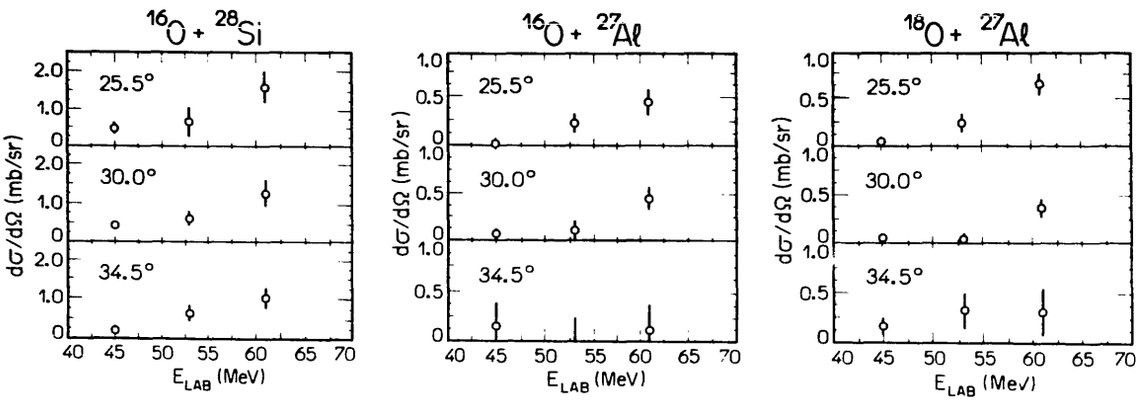

Fig. 9. Energy dependence of the break-up differential cross section $d\sigma_{BU}/d\Omega_C$ for three different detection angles of the carbon ejectile.

should supply a satisfactory description of the overall behaviour of the non-statistical process.

Using the formalism developed by Bertulani and Hussein [14]), we have for the break-up amplitude

$$T_{\mathrm{fi}} = \sum_{LM} [T^{\mathrm{N}}_{LM}(\boldsymbol{k}, \boldsymbol{k}', \boldsymbol{q}) + T^{\mathrm{C}}_{LM}(\boldsymbol{k}, \boldsymbol{k}', \boldsymbol{q})], \tag{2}$$

where $T^{\mathrm{N}}_{LM}(T^{\mathrm{C}}_{LM})$ is the L-pole component of the nuclear (Coulomb) contribution to the transition matrix. In eq. (2), $\boldsymbol{k}(\boldsymbol{k}')$ is the initial (final) relative momentum in the projectile+target centre-of-mass frame, and $\boldsymbol{q}$ is the relative momentum of the emergent fragments of the projectile in its c.m. frame.

The amplitudes T^{N}_{LM} and T^{C}_{LM} are evaluated using a slightly generalized version of the formalism of ref. [14]). The details of these calculations will be presented elsewhere [14b]). They can be expressed as products of a DWBA factor, depending on $\boldsymbol{k}$ and $\boldsymbol{k}'$, with an excitation factor, depending on Q. The DWBA-factor is evaluated using distorted waves generated by standard absorption potentials [15]). The excitation factor is a matrix element of the interaction between the initial and the final states of the projectile fragments.

Owing to the short-range nature of the nuclear form factor, T^{N}_{LM} is dominated by the monopole ($L=0$) term. On the other hand, the Coulomb amplitude is sensitive to the charge-to-mass ratio of the fragments, which is the same for the $\alpha + {}^{12}\mathrm{C}$ system (and nearly the same for $\alpha + {}^{14}\mathrm{C}$). This leads to the dominance of the $L=2$ term (the $L=0$ term is absent for Coulomb excitation). However, in our calculation the Coulomb amplitude turns out to be much smaller than its nuclear counterpart. This can be easily understood, since for low-energy collisions the Coulomb field does not have the necessary high-frequency Fourier components to induce the break-up of the projectile, e.g., for ${}^{12}\mathrm{C}+\alpha$, $Q=7.16$ MeV.

In this model, the direct break-up differential cross section (DBU) is given by

$$\frac{\mathrm{d}^2\sigma}{\mathrm{d}\Omega_\alpha \, \mathrm{d}\Omega_{\mathrm{C}}} = \frac{1}{\hbar V_{\mathrm{lab}}} \frac{m_{\mathrm{C}}}{(2\pi)^5} \int_0^\infty k^2 k_{\mathrm{C}} |T^{\mathrm{N}}_{00}(\boldsymbol{k}, \boldsymbol{k}', \boldsymbol{q})|^2 \, \mathrm{d}k_\alpha \,. \tag{3}$$

The result of calculation based on this formalism is shown in figs. 5 and 6 (solid curves). Conventional strong absorption optical potential were used to generate the distorted waves. It is clear from these figures that position and width of the main peaks are well accounted for. Notice that an overall normalization factor was used in the calculation. A discussion concerning these factors will be presented in sect. 4.2. The negative-angle tail of the correlation cross section underestimates the data. As we show in the following, this region is dominated by another process, namely, incomplete fusion.

4.2. STATISTICAL BREAK-UP

Besides the fast direct break-up process (DBU) discussed above, the nuclear system could evolve into the break-up channel via a two-step process in which the

projectile is excited to a resonant cluster state which then decays. When the resonances are excited in the projectile overlap, one anticipates the adequacy of a statistical description. We denote the T-matrix for the two-step process, schematically, as

$$T=\sum_c \int \langle \varphi_f^{(-)}|V|\psi_c^{(+)}\rangle|c^{(+)}\rangle \frac{1}{E-E_c+i\frac{1}{2}\Gamma}\langle \tilde{c}^{(+)}|\langle \tilde{\psi}_c^{(+)}|V|\psi_i^{(+)}\rangle , \tag{4}$$

where $|c\rangle$ represents the compound nucleus state and $|\psi_c^{(+)}\rangle$ the wave function that represents the relative motion of the compound nucleus with respect to the target. Then, the energy-averaged cross section becomes (for simplicity we ignore the intrinsic spins of the nuclei)

$$\frac{d^2\sigma}{d\Omega_1\, d\Omega_2}=\sum_l \tilde{P}_{\text{inel}}(\theta_1, l)\frac{T_f(l)}{\sum_j T_j(l)}(P_l(\cos\theta_2))^2 , \tag{5}$$

where θ_1 is the scattering angle of the first (inelastic) process, θ_2 is the emission angle of the compound nucleus fragment with respect to its center of mass and l, the angular momentum of the relative motion after the C.N. excitation. T is the transmission coefficient and $\tilde{P}_{\text{inel}}$ is proportional to the modulus squared of inelastic matrix element $\langle \tilde{\psi}_c^{(+)}|V|\psi_i^{(+)}\rangle$. This matrix element is related to the usual matrix element $\langle \psi_c^{(-)}|V|\psi_i^{(+)}\rangle$ by $\langle \tilde{\psi}_c^{(+)}|V|\psi_i^{(+)}\rangle=\langle \psi_c^{(-)}|S^{-1}V|\psi_i^{(+)}\rangle$ where S^{-1} is the inverse of the elastic S-matrix in channel c (the elastic scattering of the excited projectile by the target). Collecting all factors in eq. (5) one then obtains

$$\frac{d^2\sigma}{d\Omega_1\, d\Omega_2}=\sum_l P_{\text{inel}}(\theta_1, l)\left(\frac{1}{1-T_c(l)}\right)\frac{T_f(l)}{\sum_j T_j(l)}P_l(\cos\theta_2) . \tag{6}$$

In obtaining this expression, it was assumed that the transmission coefficient representing absorption in $|\psi_c^{(+)}\rangle$ is approximately equal to those of the Hauser-Feshbach cross section for the compound nucleus c. We note that the lth cross section is window-like, as expected for peripheral processes.

4.3. INCOMPLETE FUSION

We note here that the formalism described in sect. 4.2 can also be applied either to a statistical break-up process (SBU) as identified in line (b) of expression (1) or to an incomplete fusion process (ICF) ((c) in the same expression). In this case, part of the projectile is transferred to the target to form a compound nucleus, which then decays. The probability $P_{\text{inel}}(l)$ is then replaced by the transfer probability $P_{\text{trans}}(l)$ and the transmission coefficients then refer to the target + participant system instead of projectile + participant as in the SBU process. As mentioned earlier, we will consider only ICF the case in which an α-particle is transferred from the projectile to the target, and then reemitted, i.e. case (c) in expression (1). The results

are shown in fig. 7. Case (d) in which a carbon cluster is transferred and reemitted will be neglected due to the very low values of the transmission coefficient T_j (l), where j stands in this case for C+Si (Al).

5. Results and conclusions

Calculations based on the DBU model, presented in figs. 5 and 6, carry an overall normalization factor (N). However, it should be stressed that, for a given system, the normalization factor is constant for all energies and carbon detection angles (see fig. 5). When different systems are compared, (see figs. 5a, 6a and 6b), the value of N varies by less than a factor of 2. According to these results, we can conclude that the predictions of the DBU model account satisfactorily for the angular correlation position and width as well as for the cross-section energy dependence. This, however, does not imply that the data are completely consistent with a fast break-up process, owing to our need of the normalization factor. This factor stems partly from the use of DWBA instead of coupled channels and partly from the fact that slower two-step processes are also present. We now turn to the description of this latter contribution.

In order to perform, in a simple way, the calculations based on the statistical break-up model (SBU) as well as the incomplete fusion model (ICF), standard computer codes were used for the evaluation of the inelastic-excitation probability (PTOLEMY) [16]) and statistical decay of the compound-nucleus cross section (STATIS) [17]). The adopted procedure, in this case, is similar to the one used in ref. [6]). For the projectile inelastic scattering, cluster states in ^{16}O(^{18}O) were included implicitly in the calculation. All the known discrete states in the residual nuclei were considered in the Hauser-Feshbach calculations for the statistical decay of the compound nucleus. In the case of α-transfer and reemission, the observed ^{12}C particles are produced in the first step. Consequently, their momenta define exactly the direction and excitation energy of the associated compound nucleus ^{31}P* (^{32}S*). Here, instead of calculating the DWBA probability for α-transfer, experimental yields (from the ^{12}C spectra) were used as was done in ref. [6]). Thus the main difference with respect to the use of partial-l probabilities product and partial-l cross sections described in expression (5) is that crossed terms in l are included in ref. [6]) and absent in eq. (5).

The justification for this procedure lies entirely in the fact that existing DWBA and Hauser-Feshbach codes supply cross-section values and, further, one anticipates on general grounds that these cross-terms contribute at most values which are about a factor Δ_l / l_g smaller than the diagonal terms. Here Δ_l is the l-space diffuseness of a typical transmission coefficient and l_g is the grazing angular momentum.

In the case of statistical break-up (SBU), due to the fact that the observed ^{12}C nuclei are produced in the second step, the inclusive projectile excitation probabilities were obtained by DWBA calculations.

From our results (i.e. E^{rel} values and fits to the angular correlations) it is clear that the yield to negative backward angles is dominated by the incomplete-fusion process with a threshold at $E_{lab}(0) \simeq 45$ MeV. The forward angles are dominated by break-up processes with its threshold at $E_{lab} \simeq 40$ MeV. The position of the angular correlation peak is mostly sensitive to the direction of the ^{12}C particle as well as to the average energy deposited in the excitation of the projectile. Therefore, the geometry of such an experiment is very important in shaping the angular correlation in the sense that the dynamics here play a minor role. This feature is clearly exhibited from the equally good fits that both the DBU and the SBU models supply to the data.

References

1) P.L. Gonthier, M. Ho, M.N. Namboodiri, J.B. Natowitz, L. Adler, S. Simon, K. Magel, S. Kniffer and A. Khodai, Nucl. Phys. **A411** (1983) 289
2) M. Bini, C.K. Gelbke, D.K. Scott, T.J.M. Symons, P. Doll, D.L. Hendrie, J.L. Laville, J. Mahoney, M.C. Hermaz, C. Olmer, K. van Bibber and H.H. Wieman, Phys. Rev. **C22** (1980) 1945
3) W.D.M. Rae, A.J. Cole, B.G. Harvey and R.G. Stokstad, Phys. Rev. **C30** (1984) 158
4) J.W. Harris, T.M. Cormier, D.F. Geesaman, L.L. Lee Jr., R.L. McGrath and P.J. Wurm, Phys. Rev. Lett. **38** (1977) 1460
5) M.B. Tsang, W.G. Lynch, R.J. Puigh, R. Vandenbosh and A.G. Seamster, Phys. Rev. **C23** (1981) 1560
6) N. Carlin, M.M. Coimbra, N. Added, R.M. dos Anjos, L. Fante Jr., M.C.S. Figueira, V. Guimarães, E.M. Szanto, A. Szanto de Toledo and O. Civitarese, Phys. Rev. **C40** (1989) 91
7) S.J. Padalino and L.C. Dennis, Phys. Rev. **C31** (1985) 1794
8) S.J. Padalino, M.A. Putnam, J.A. Constable, T.G. De Clerck, L.C. Dennis, R. Zingarelli, R. Kline and K. Sartor, Phys. Rev. **C41** (1990) 594
9) M. Sasagase, M. Sato, S. Hanashima, K. Furuno, Y. Magashima, Y. Tagishi, S.M. Lee and T. Mikumo, Phys. Rev. **C27** (1983) 2630
10) O. Sala and G. Spalek, Nucl. Instr. Meth. **122** (1974) 213
11) N. Added, PhD Thesis, University of São Paulo, Brazil (1991) (unpublished)
12) B.W. Hooton, J.M. Freeman and P.P. Kane, Nucl. Instr. Meth. **124** (1975) 29
13) S.L. Tabor, L.C. Dennis, K.W. Kemper, J.D. Fox, K. Aldo, G. Neushaefer, D.G. Kovar and H. Ernst, Phys. Rev. **C24** (1981) 960;
S.L. Tabor, L.C. Dennis and K. Abdo, Phys. Rev. **C24** (1981) 2552
14) C.A. Bertulani and M.S. Hussein, Nucl. Phys. **A524** (1991) 306;
C.A. Bertulani, L.F. Canto and M.S. Hussein, to be published
15) J. Cramer, R.M. Devries, D.A. Goldberg, M.S. Zisman and C.F. Maguire, Phys. Rev. **C14** (1976) 2158
16) S.C. Pieper and MacFarlaine, Ptolemy-DWBA CODE, Argonne National Laboratory, USA (1976) (unpublished)
17) R.G. Stokstad, Yale University Wright Nuclear Structure Laboratory Report **59** (1972)